A first-principles DFT+GW study of spin-filter and spin-gapless semiconducting Heusler compounds

M. Tas^a, E. Şaşıoğlu^{b,1}, C. Friedrich^b, I. Galanakis^a

^aDepartment of Materials Science, School of Natural Sciences, University of Patras, GR-26504 Patra, Greece

Abstract

Among Heusler compounds, the ones being magnetic semiconductors (also known as spin-filter materials) are widely studied as they offer novel functionalities in spintronic and magnetoelectronic devices. The spin-gapless semiconductors are a special case. They possess a zero or almost-zero energy gap in one of the two spin channels. We employ the GW approximation to simulate the electronic band structure of these materials. Our results suggest that in most cases the use of GW self energy instead of the usual density functionals is important to accurately determine the electronic properties of magnetic semiconductors.

Keywords: Fully-compensated ferrimagnetic Heusler compounds, Magnetic semiconductors, Spin-gapless semiconductors PACS: 75.47.Np, 75.50.Cc, 75.30.Et

1. Introduction

Spintronics and magnetoelectronics constitute one of the most rapidly expanding research fields of materials science and condensed matter physics [1]. The on-going research on the modelling of novel materials plays a key role in the advancements in this research field as it allows an à-la-carte design of materials for specific applications [2]. In this respect, Heusler compounds [3, 4, 5] are widely studied due to the variety of magnetic properties exhibited, in particular, in combination with the half-metallicity [6, 7, 8, 9, 10, 11, 12]. Apart from half-metallic Heusler compounds, also the ones being magnetic semiconductors are of interest for spintronics and magnetoelectronics [13]. Magnetic semiconductors can act as spin-filter materials (SFMs) [14, 15] to maximize the efficiency of devices based on magnetic tunnel junctions (MTJs) [16, 17, 18, 19], like the

^bPeter Grünberg Institut and Institute for Advanced Simulation, Forschungszentrum Jülich and JARA, 52425 Jülich, Germany

Email addresses: tasm236@gmail.com (M. Tas), ersoy.sasioglu@physik.uni-halle.de (E. Şaşıoğlu), galanakis@upatras.gr (I. Galanakis)

¹Present address: Institut für Physik, Martin-Luther-Universität Halle-Wittenberg, D-06099 Halle (Saale), Germany

recently proposed spin-current diodes [20]. A special class of magnetic semiconductors are the so-called spin-gapless semiconductors (SGSs), where one of the two spin channels presents a gapless or almost-gapless semiconducting behavior while the other spin channel possesses a finite gap at the Fermi level [21, 22, 23].

Several studies have been devoted recently to the SFMs and SGSs. First-principles electronic band structure calculations have suggested that the ordered quaternary (CoV)YAl and (CrV)YAl Heusler compounds [24, 25] - where Y stands for Ti, Zr, or Hf - are SFMs [26, 27, 28, 29]. The former compounds are ferromagnetic semiconductors, while the latter ones are fully-compensated ferrimagnetic semiconductors, as they combine the existence of energy gaps in both spin directions to zero magnetization [26, 27]. Both families of Heusler SFMs present high Curie temperatures well above the room temperature and, thus, are of interest for room-temperature spintronic/magnetoelectronic applications contrary to other well known SFMs [30, 31, 32, 33]. The fully-compensated ferrimagnetic character of (CrV)YAl compounds makes them even more attractive for applications as the zero net magnetization leads to vanishing stray fields and thus to minimal energy losses. Recently, Stephen and collaborators have successfully grown samples of (CrV)TiAl and their measurements confirmed the ab-initio predictions [34].

SGS materials are known for almost a decade [35, 36, 37, 38]. Although several ab-initio calculations had suggested that the band structure of Mn₂CoAl, an inverse Heusler compound [39], is compatible with that of an SGS material [40, 41, 42], it was not until 2013 when experiments by Ouardi et al. confirmed the SGS character of Mn₂CoAl in bulk-like polycrystalline films and measured a Curie temperature of 720 K far above the room temperature [22]. Also, experiments were carried out on thin films of Mn₂CoAl on various substrates; films on top of GaAs were found to deviate from SGS [43, 44], while films on thermally oxidized Si substrates were found to be SGS with a Curie temperature of 550 K [45]. These experimental findings were accompanied by several ab-initio calculations [29, 24, 46, 47, 48, 49, 50, 51, 52], and also Ti₂CoSi, Ti₂MnAl, Ti₂VAs and Cr₂ZnSi have been identified as potential SGS materials sublattices [46]. Simultaneously, several theoretical studies appeared dealing with the various phenomena that affect the SGS character of these compounds with a focus mainly on Mn₂CoAl [53, 54, 55, 56].

2. Motivation and computational details

For SGS materials the most important property is the zero gap in the majority-spin or spin-up (for materials with zero magnetization where we cannot distinguish majority and minority spins) electronic band structure. In the case of SFMs the most important property is the energy difference in the bottom of the conduction band for the two spin directions, the exchange splitting $2\Delta E_{\rm ex}$, which corresponds to the difference of the barrier that spin up and spin down electrons confront when they tunnel through the SFM [57]. This exchange splitting for the SFMs under study is about 0.1-0.3 eV [26, 27]. Thus, the energy quantities characterizing the SGSs and SFMs are relatively small.

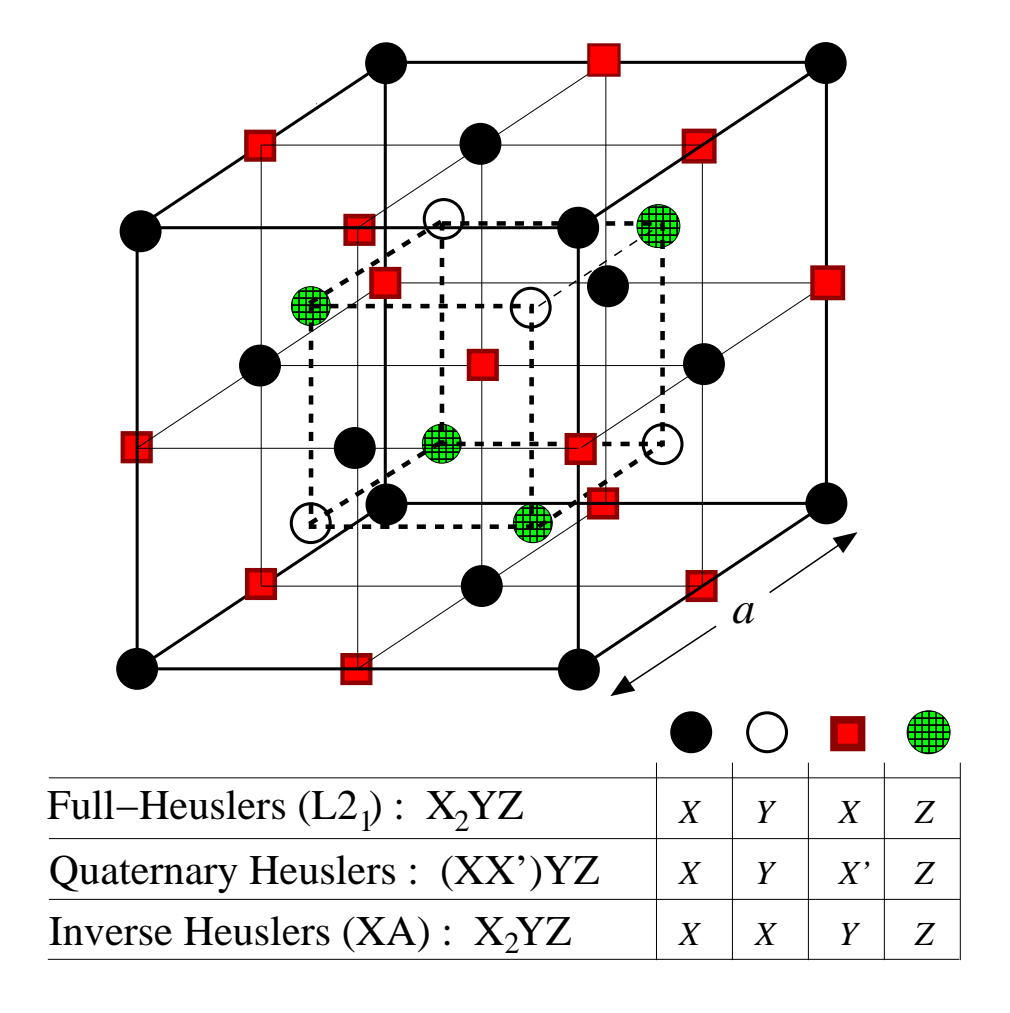


Figure 1: (Color online) Schematic representation of the lattice structure of the full-Heusler compounds adopting the $L2_1$ lattice structure, the quaternary ordered ones, which include also the spin-filter materials, and the inverse Heusler compounds adopting the XA (also known as X_a) lattice structure which is identical to that of the spin-gapless semiconducting Heusler compounds. In all cases, the lattice consists of four interpenetrating fcc lattices.

Table 1: For the spin-filter and spin-gapless semiconducting materials we present the used theoretical lattice constants a (in Å) from references [26, 27, 46] with the exception of Mn₂CoAl where we have used the experimental value from reference [22], the magnetic energy ΔE_M in eV defined as the difference between the magnetic and the non-magnetic calculations, the atom-resolved spin magnetic moments (in μ_B), the total spin magnetic moment $m^{f.u.}$ (in μ_B), and the exchange splitting $2\Delta E_{\rm ex}$ (in eV) obtained from both the PBE functional and the GW self-energy (all other quantities are computed using PBE only).

(XX')YZ	a(Å)	ΔE_M	m^{X}	$m^{\mathrm{X}'}$	m^{Y}	m^{Z}	$m^{\mathrm{f.u.}}$	$2\Delta E_{\mathrm{ex}}^{\mathrm{PBE}}$	$2\Delta E_{\mathrm{ex}}^{GW}$
(CoV)TiAl	6.04	-0.66	0.249	2.162	0.279	0.023	3.0	0.04	0.14
(CoV)ZrAl	6.26	-0.77	0.147	2.329	0.168	0.018	3.0	0.25	0.18
(CrV)TiAl	6.20	-0.78	-2.740	2.092	0.417	0.023	0.0	0.29	0.28
(CrV)ZrAl	6.41	-0.91	-2.913	2.362	0.251	0.043	0.0	0.27	0.26
X_2YZ	a(Å)	ΔE_M	m^{X^A}	m^{X^B}	m^{Y}	m^{Z}	$m^{\mathrm{f.u.}}$	$2\Delta E_{ m ex}^{ m PBE}$	$2\Delta E_{\mathrm{ex}}^{GW}$
Cr_2ZnSi	5.85	-0.11	-1.58	1.62	0.03	-0.06	0.0	0.28	0.52
Mn_2CoAl	5.798	-0.95	-1.72	2.75	1.04	-0.04	2.0	0.34	0.36
Ti_2CoSi	6.03	-0.36	1.41	0.71	0.40	0.05	3.0	0.11	0.02
${ m Ti}_2{ m MnAl}$	6.24	-0.30	1.13	1.00	-2.59	0.04	0.0	0.43	0.42

The fact that we have to deal with such small energy differences calls for a sophisticated theoretical method for the description of the electronic excitation spectrum or, in other words, the band structure of these materials. While being very successful for ground-state properties, standard DFT functionals are not adequate for this purpose. This is not a failure of the approximations but rather because the Kohn-Sham eigenvalues are not meant to be interpreted as the excitation energies of the real interacting system. Technically, these eigenvalues are the excitation energies of an unphysical, auxiliary system of non-interacting electrons, the Kohn-Sham system. As a consequence, they miss renormalization effects due to electronic exchange and correlation effects. Therefore, we employ in the present study the GW approximation for the electronic self-energy, which is derived in the framework of many-body perturbation theory and, thus, treats the interactions among the electrons beyond the mean-field approximation [58]. It contains the electronic exchange exactly and a large part of electronic correlation. This approach is well known to have a strong effect on the band gaps of semiconductors and insulators [59]. In particular, the GW approach corrects the band gaps from their (usually underestimated) DFT values towards experiment. Furthermore, it is known to produce more accurate results for halfmetallic Heusler compounds than other simplified approaches such as GGA+U[60, 61]. For the half-metallic Heusler compounds Co₂MnSi and Co₂FeSi, it has also been shown to be able to accurately reproduce the experimental photoemission and x-ray absorption spectra [62]. Thus, we expect the GW self-energy to play an important role in the theoretical description of the SFM and SGs materials; this assumption is confirmed by our results in the next two sections.

We have chosen as SFMs the ferromagnetic (CoV)TiAl and (CoV)ZrAl semiconductors [26] and the fully-compensated ferrimagnetic (CrV)TiAl and (CrV)ZrAl semiconductors [27]. As SGS materials to study, we have chosen

Mn₂CoAl and Ti₂CoSi which present a ferrimagnetic and ferromagnetic configuration, respectively, with a non-zero net magnetization, as well as Cr₂ZnSi and Ti₂MnAl which are fully-compensated ferrimagnets [46]. The lattice structure of all compounds under study is presented in figure 1. The lattice has a fcc structure with four atoms as basis along the diagonal. In the usual full-Heusler compounds having the chemical formula X₂YZ, the sequence of the atoms is X-Y-X-Z. For the quaternary Heuslers like the SFMs under study, having the chemical formula (XX')YZ the sequence of the atoms is X-Y-X'-Z. Finally, for the so-called inverse Heuslers, which have the same chemical formula as the usual full-Heuslers with a larger valence on Y than on X, like in the studied SGS, the sequence of the atoms changes and it is now X-X-Y-Z (we use the superscripts A and B to distinguish the two non-equivalent X atoms). For all cases we have used the theoretical equilibrium lattice constants determined in references [26, 27, 46] and shown in table 1, with the exception of Mn₂CoAl where we have used the experimental lattice constant in reference [22].

As a first step we performed simulations using the standard density-functional-theory (DFT) based on the full-potential linearized augmented-plane-wave (FLAPW) method as implemented in the FLEUR code [63] within the generalized-gradient approximation (GGA) of the exchange-correlation potential as parameterized by Perdew, Burke and Ernzerhof (PBE) [64]. By using the PBE results as an input, we performed calculations employing the GW approximation using the SPEX code [65]. Details of the calculations are identical to the ones in references [66, 67], where non-magnetic semiconducting and antiferromagnetic semiconducting Heusler compounds were studied, respectively.

3. Results on the spin-filter materials

We begin our discussion with the SFMs. We have examined first, the stability of the magnetic states by calculating the energy difference between the magnetic and the non-magnetic states, ΔE_M , using the PBE functional, see table 1. For all four SFMs under study the obtained values are negative and thus the magnetic state is favorable. Moreover, the calculated values range between -0.66 eV for (CoV)TiAl down to -0.91 eV for (CrV)ZrAl. These values are in perfect agreement with the calculated values in references [26] and [27] where a different electronic structure method was employed, the full-potential nonorthogonal local-orbital minimum-basis band structure scheme (FPLO) [68]. Thus, these compounds should exist at least as metastable structures as also suggested by the experiment in [34].

Second, using the PBE functional, we have calculated the atom-resolved spin magnetic moments as well as the total spin magnetic moment per formula unit (f.u.) which coincides with the per unit cell value and we present these results also in table 1. For the two compounds containing Co, the total spin magnetic moment is 3 $\mu_{\rm B}$, while for the two Cr-based compounds the calculated total spin magnetic moment is exactly zero in agreement with the calculations in references [26] and [27]. The Ti atoms in all four compounds carry a small spin magnetic moment being ferromagnetically coupled to the spin magnetic

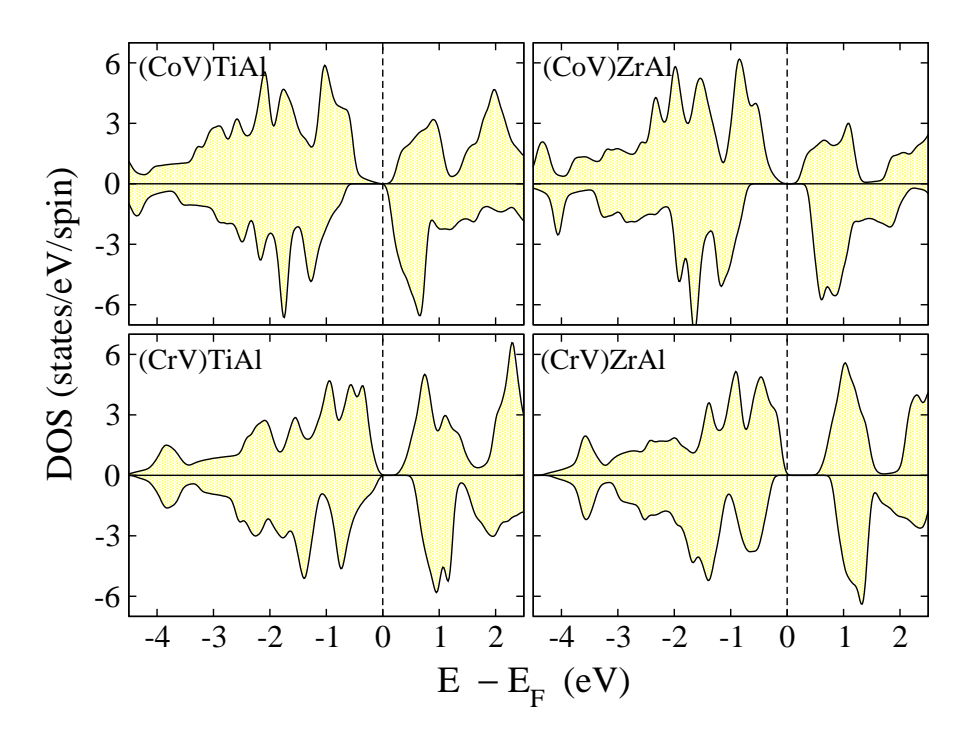


Figure 2: (Color online) Density of states for all four SFMs under study obtained from the PBE approximation. The zero energy value denotes the Fermi level. Positive(negative) DOS values correspond to the spin-up(spin-down)electrons.

moment of the V atoms which range from about $2.1~\mu_{\rm B}$ to about $2.4~\mu_{\rm B}$. In the case of (CoV)TiAl and (CoV)ZrAl the spin magnetic moments of the Co atoms are also ferromagnetically coupled to the spin magnetic moments of the V atoms leading to a ferromagnetic state. On the contrary, in the case of (CrV)TiAl and (CrV)ZrAl compounds the Cr atoms carry very large negative spin magnetic moments approaching -3 $\mu_{\rm B}$, which balance the positive spin magnetic ground state. The origin of this coupling can be easily explained using the phenomenological Bethe-Slater rule as discussed in reference [27]. The atom-resolved spin magnetic moments here are also similar to the values calculated in references [26] and [27]; the only noticeable difference being that the absolute values of the spin magnetic moments are slightly smaller.

The density of states (DOS) shown in figure 2 for all four SFMs under study is compatible with a magnetic semiconducting ground state in agreement with the FPLO results in references [26] and [27]. In the last columns of table 1 we have compiled the exchange splittings obtained from PBE and GW. For (CrV)TiAl and (CrV)ZrAl both approximations yield similar values with a difference of only 0.01 eV. Also the calculated values for these two Cr-based compounds are identical to the values of 0.28 and 0.25 eV calculated in reference [27]. The discrepancy between the GW and the PBE calculations is larger for the case of (CoV)TiAl and (CoV)ZrAl compounds. For the first compound GW increases the exchange splitting by 0.1 eV while for the second compound it decreases by 0.07 eV. We have to note here that the present calculations using PBE yield, with respect to the PBE calculations in reference [26], half the exchange splitting energy for (CoV)TiAl. On the contrary, the present first-principles calculations using the PBE functional yield for (CoV)ZrAl an exchange splitting identical to the calculated value in reference [26]. Our GW results suggest that (CrV)TiAl and (CrV)ZrAl are more suitable for applications since the large values of the exchange splitting ensure a more efficient spin-dependent tunnelling in realistic devices [14, 15].

In figures 3 and 4 we present the spin-resolved band structure for (CoV)TiAl and (CrV)TiAl using both the PBE functional (red dashed line) and the GW approximation (solid blue line). Note that for (CrV)TiAl both spin directions have the same population of electrons and thus arbitrarily we denote as majority-spin band the one with the smallest energy band gap which corresponds to the negative spin magnetic moment of the Cr atoms in table 1. The Fermi level is set to be the top of the valence band of the majority-spin electrons. While for the Heusler compounds studied in references [66] and [67] GW only marginally affected the bands close to the Fermi level, in the case of SFMs GW has a more profound effect on the bands just above and below the Fermi level. Most of the bands around the Fermi level are shifted away from the Fermi level leading to larger band gaps. This shift is quantified for all compounds under study in the first column of table 2, where we present for all four compounds and for both spin directions the band gap using both the GW approximation and the PBE functional in parenthesis. The largest change in percentage is observed for the majority-spin band of (CoV)ZrAl where the band gap within GW is doubled

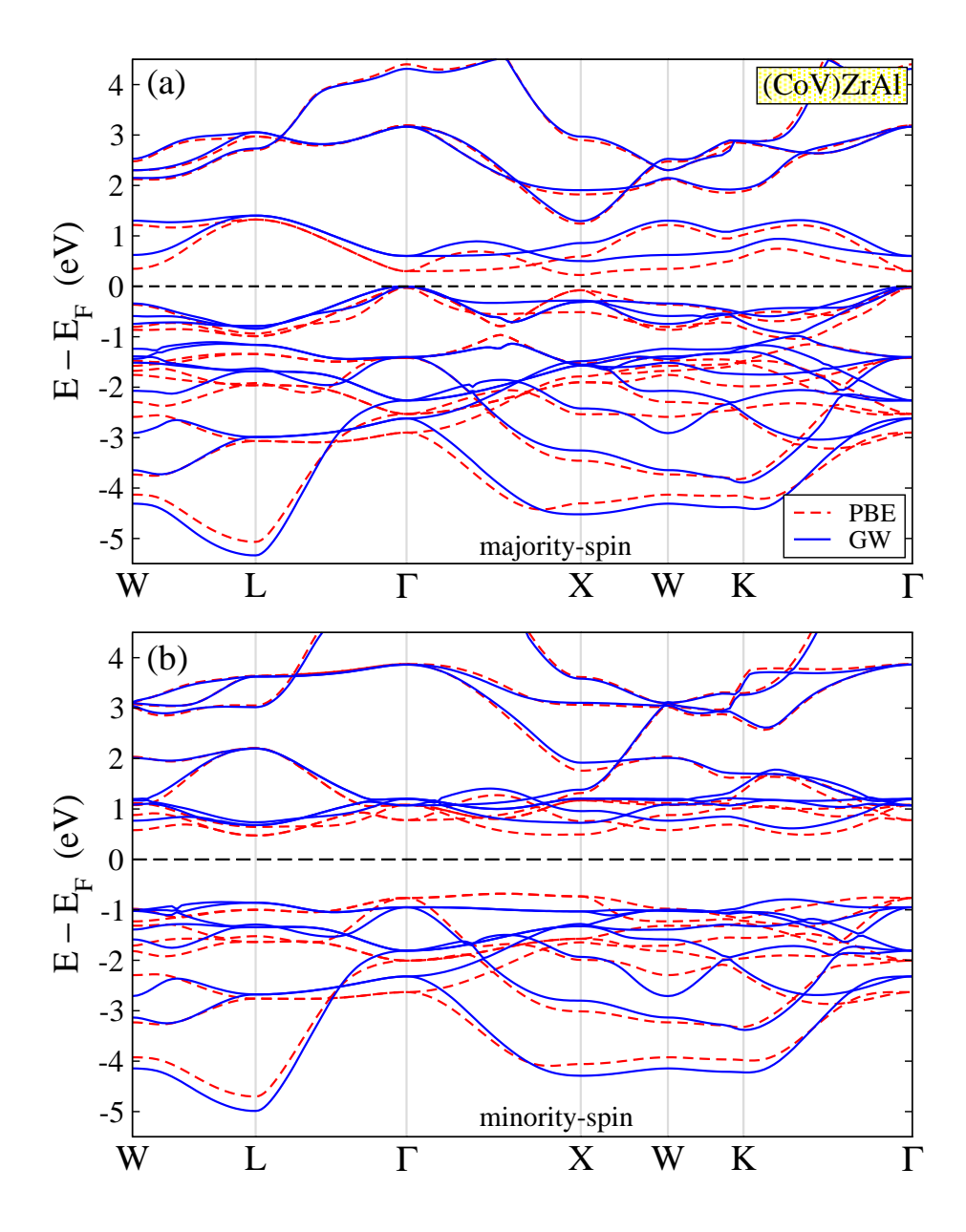


Figure 3: (Color online) Spin-resolved electronic band structure of (CoV)TiAl along the high-symmetry directions in the first Brillouin obtained from PBE (red dashed line) and GW (blue solid line) approximations. The zero energy value denotes the Fermi level.

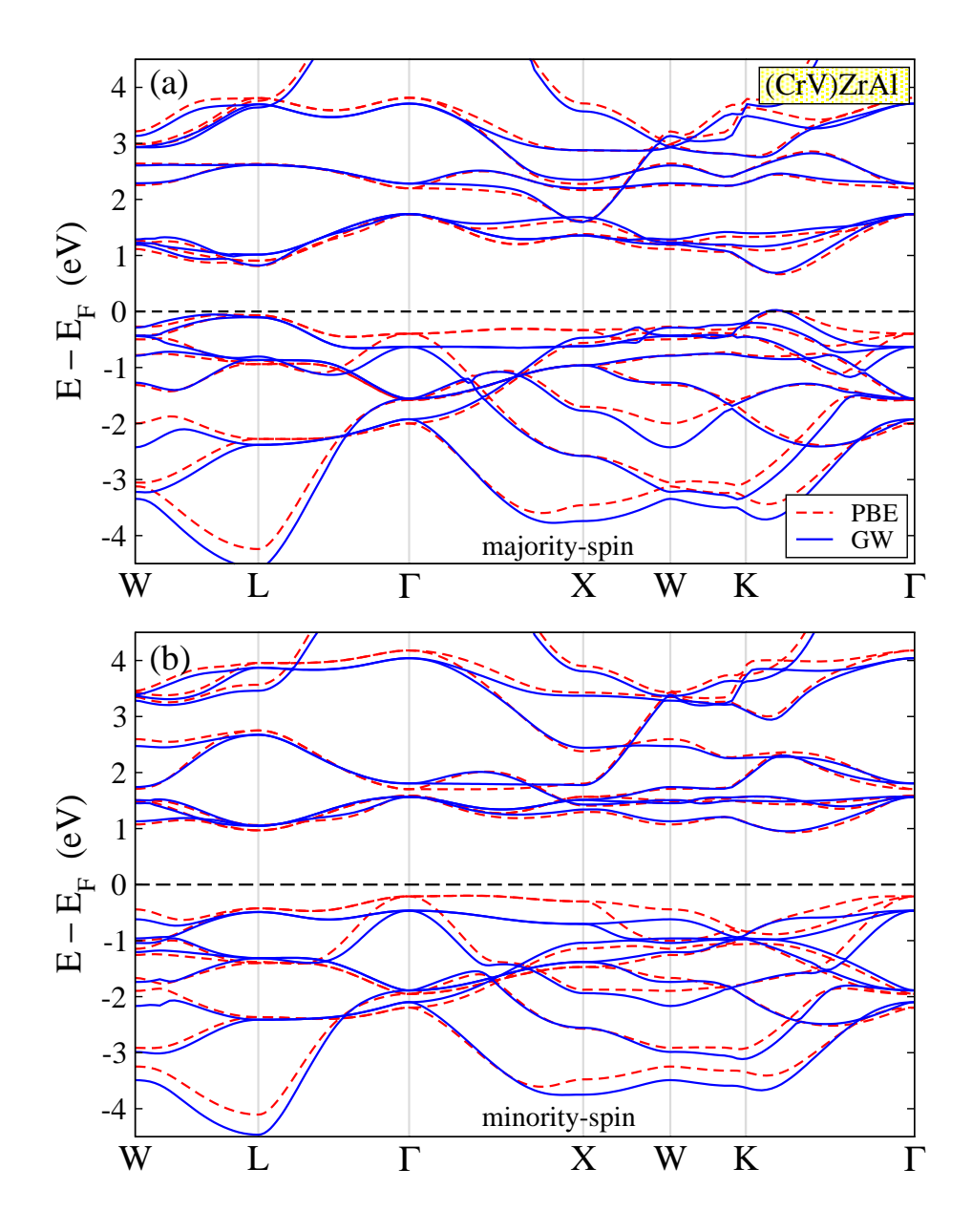


Figure 4: (Color online) Same as figure 3 for (CrV)TiAl.

Table 2: Calculated PBE (in parenthesis) and GW energy band gaps and transition energies (all in eV) between certain high-symmetry points for both spin channels of the spin-filter materials under study. For the case of fully-compensated ferrimagnets, where spin-up and spin-down bands have the same population, we choose as majority-spin band structure the one with the smallest energy band gap (E_g) .

(XX')YZ	$\mathrm{E}_\mathrm{g}^{GW}(\mathrm{E}_\mathrm{g}^\mathrm{PBE})$	$\Gamma \to \Gamma$	$X \rightarrow X$	$L{\rightarrow}L$	$\Gamma \rightarrow X$	$\Gamma \to L$	$X{ ightarrow}L$			
	Majority-Spin Band-Structure									
(CoV)TiAl	0.44(0.23)	0.51(0.31)	1.21(0.74)	2.28(2.24)	0.44(0.23)	1.29(1.21)	2.06(1.71)			
(CoV)ZrAl	0.50(0.25)	0.60(0.33)	0.80(0.30)	2.24(2.26)	0.50(0.25)	1.40(1.35)	1.71(1.40)			
(CrV)TiAl	0.45(0.37)	2.02(2.05)	1.79(1.54)	1.08(1.00)	1.33(1.30)	0.98(0.94)	1.44(0.94)			
(CrV)ZrAl	0.66(0.66)	2.37(2.13)	1.97(1.71)	0.92(0.88)	1.98(1.78)	1.45(1.21)	1.44(1.44)			
		Minority-Spin Band-Structure								
(CoV)TiAl	0.96(0.80)	1.63(1.34)	2.06(1.51)	1.60(1.48)	1.43(1.21)	1.09(0.88)	1.73(1.18)			
(CoV)ZrAl	1.53(1.15)	2.01(1.54)	1.75(1.23)	1.53(1.47)	1.67(1.26)	1.63(1.24)	1.70(1.21)			
(CrV)TiAl	0.81(0.70)	1.56(1.55)	2.08(1.70)	1.56(1.40)	1.25(1.20)	0.94(0.78)	1.77(1.27)			
(CrV)ZrAl	1.42(1.14)	2.02(1.80)	2.04(1.60)	1.54(1.39)	1.80(1.50)	1.51(1.18)	1.75(1.27)			

from 0.25 eV to 0.50 eV, and the largest change in absolute values is in the minority spin band structure of the same compound where GW increases the gap by 0.38 eV from 1.15 eV to 1.53 eV. The only exception in the behavior is the majority spin band structure of (CrV)ZrAl where the band gap is 0.66 eV using both GW and PBE. The effect of the GW renormalization is even more important for the transition energies shown in table 2 as well. For example, in the majority spin band structure of (CoV)ZrAl the **k**-conserved transition energy from the valence to the conduction band at the X point is 0.30 eV in PBE, but it increases to 0.80 eV using the GW approximation. Thus, one may conclude that correlations play an important role in spin-filter Heusler compounds and the use of more sophisticated schemes than the simple density functionals is needed to correctly describe their electronic band structure properties.

4. Results on spin-gapless semiconductors

In the second part of our study, we focus on the SGS materials, namely $\rm Cr_2ZnSi$, $\rm Mn_2CoAl$, $\rm Ti_2CoSi$, and $\rm Ti_2MnAl$. The magnetic moments and the exchange splitting can be found in table 1. The calculated magnetic energy (difference between the total energy for a spin-polarized and a non-spin-polarized calculation) suggests that these compounds prefer the magnetic configuration and especially for $\rm Mn_2CoAl$, which is the prototype the value approaches -1 eV, and this explains why this was the first SGS Heusler to be grown. Only $\rm Cr_2ZnSi$ has a very small magnetic energy of -0.11 eV and thus would be more difficult to stabilize its magnetic phase in experiments. The spin magnetic moments have been already presented in detail in reference [56]. Thus, we will only shortly discuss them here. The most noticeable difference between this study and the one in reference [56] is that for $\rm Mn_2CoAl$ we have used the experimental lattice constant of 5.798 Å, while in [56] the equilibrium lattice constant of 5.73

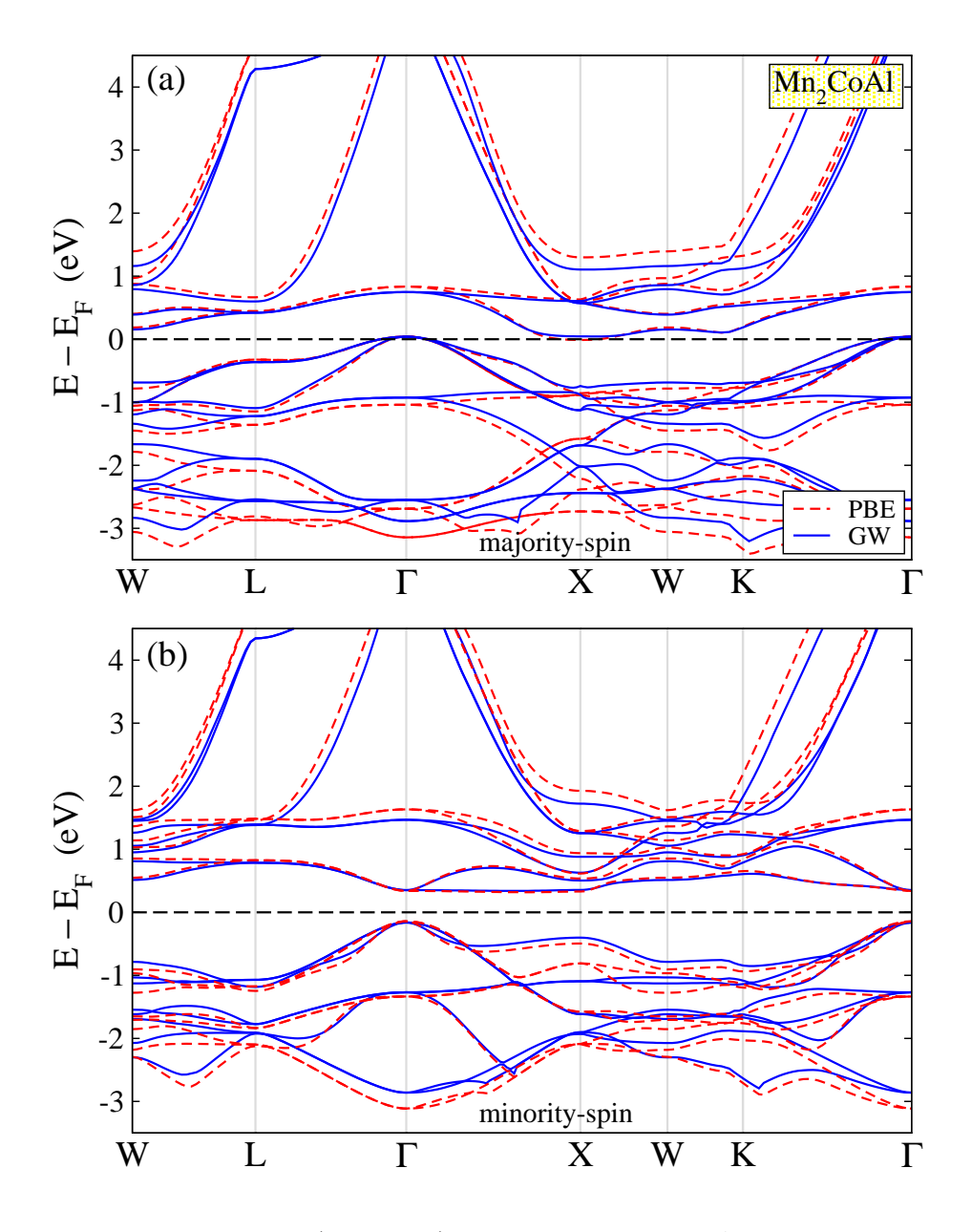


Figure 5: (Color online) Same as figure 3 for $\rm Mn_2CoAl.$

Table 3: Same as table 2 for the spin-gapless semiconductors.

(XX')YZ	$\mathrm{E}_\mathrm{g}^{GW}(\mathrm{E}_\mathrm{g}^\mathrm{PBE})$	$\Gamma \to \Gamma$	$X \rightarrow X$	$L{ ightarrow}L$	$\Gamma \to X$	$\Gamma \to L$	$X{ ightarrow}L$			
	Majority-Spin Band-Structure									
$\mathrm{Cr_{2}ZnSi}$	0.00(0.00)	3.23(3.27)	$1.\overline{21(1.32)}$	0.00(0.00)	2.01(1.81)	1.71(1.67)	0.91(1.17)			
Mn_2CoAl	0.02(0.05)	0.72(0.79)	0.79(0.84)	0.79(0.77)	0.02(-0.05)	0.39(0.40)	1.17(1.30)			
Ti_2CoSi	0.13(0.00)	0.54(0.36)	0.35(0.32)	2.15(2.11)	0.13(0.00)	1.45(1.42)	1.67(1.73)			
$\mathrm{Ti_{2}MnAl}$	-0.01(0.07)	2.08(2.20)	1.10(1.25)	0.79(0.77)	1.21(1.28)	0.86(0.91)	0.75(0.88)			
	Minority-Spin Band-Structure									
$\mathrm{Cr_{2}ZnSi}$	0.31(0.44)	2.60(2.94)	$0.\overline{71(1.08)}$	0.31(0.44)	1.50(1.67)	1.45(1.65)	0.67(1.06)			
Mn_2CoAl	0.53(0.47)	0.52(0.48)	0.77(0.82)	1.86(2.00)	0.53(0.47)	0.96(0.97)	1.20(1.32)			
${\rm Ti_2CoSi}$	0.92(0.79)	1.69(1.42)	2.06(2.05)	1.80(1.72)	1.35(1.20)	1.16(0.97)	1.86(1.83)			
${ m Ti}_2{ m MnAl}$	0.67(0.61)	1.29(1.09)	1.70(1.30)	1.76(1.64)	0.67(0.63)	0.73(0.60)	1.75(1.28)			

Å was employed. The larger experimental lattice constant leads to spin magnetic moments of larger absolute values, but the total spin magnetic moment per formula unit remains equal to 2 $\mu_{\rm B}$ and Mn₂CoAl is a SGS for both lattice constants. The exchange splitting values presented in the last column of table 1 are of more interest. SGS materials can also act as spin filters since they are just a special case of magnetic semiconductors. With the exception of Ti₂CoSi, the SGSs under study present exchange splitting energies much larger than the SFMs studied in the previous section. For Mn₂CoAl and Ti₂MnAl the use of GW instead of PBE has a minimal effect on the obtained values contrary to the other two materials. For Ti₂CoSi, GW produces an almost vanishing exchange splitting, while for Cr₂ZnSi GW almost doubles the exchange splitting with respect to the PBE.

In figure 5 we present the spin-resolved band structure for Mn₂CoAl using both the PBE functional and the GW approximation. Contrary to (CoV)TiAl and (CrV)TiAl presented in figures 3 and 4, the situation for Mn₂CoAl is completely different. Close to the Fermi level, GW has a minimal effect on the band structure for both spin directions, and hence the energy band gaps and the transition energies presented in table 3 are only marginally affected. The majority spin band gap is 0.02 eV within GW and 0.05 eV within PBE, and the SGS character is conserved. In the minority spin band structure the GW calculated band gap is just 0.06 eV larger than the PBE one. Similarly for the transition energies for Mn₂CoAl, the discrepancy between the PBE and GW calculated values is marginal, especially for the majority-spin band structure. The other three compounds show a similar behavior. In the two compounds containing Ti atoms (Ti₂CoSi and Ti₂MnAl) GW slightly enlarges the band gaps and the transition energies, similarly to the case of the SFMs. In the case of Cr₂ZnSi the situation is opposite, and the GW renormalization slightly decreases the energy band gaps, especially for the minority-spin band structure. Overall, in the case of the SGS materials, the GW self-energy has only a small effect on the electronic band structure, but it may affect the exchange splittings significantly with consequences for spin-filter related applications.

5. Conclusions

The GW approximation for the electronic self-energy was employed to account for many-body exchange-correlation effects as a correction to standard density-functional theory calculations using the PBE functional. We have studied the properties of two distinct subfamilies of the full-Heusler compounds: (i) the ordered quaternary (also known as LiMgPdSn-type) Heusler compounds having the chemical formula (CoV)YAl and (CrV)YAl, where Y is Ti or Zr, and which are magnetic semiconductors (known as spin-filter materials), and (ii) the so-called inverse Heusler compounds with the chemical formula X₂YZ which are spin-gapless semiconductors and thus present a gapless or almost-gapless semiconducting behavior in the majority spin band structure combined with a finite energy gap in the other spin channel.

Our first-principles results suggest that the use of GW is important for the spin-filter materials. It shifts both valence and conduction bands away from the Fermi level leading to larger energy band gap values as well as larger transition energies. On the other hand, the effect of employing GW is smaller in the spin-gapless semiconductors and the usual density-functional theory gives a fair description of the properties of these materials.

Thus the effect of the GW approximation is material-specific even among materials of the same family with similar electronic and magnetic properties and its use seems essential to get a good description of their electronic properties. We hope that our results further enhance the interest in these classes of Heusler compounds and that they contribute to the understanding of their extraordinary properties.

References

References

- [1] I. Žutić, J. Fabian, and S. Das Sarma, Rev. Mod. Phys. 76 (2004) 323.
- [2] K. Sato, L. Bergqvist, J. Kudrnovsky, P.H. Dederichs, O. Eriksson, I. Turek, B. Sanyal, G. Bouzerar, H. Katayama-Yoshida, V.A. Dinh, T. Fukushima, H. Kizaki, R. Zeller, Rev. Mod. Phys. 82 (2010) 1633.
- [3] F. Heusler, Verh. Dtsch. Phys. Ges. 12, 219 (1903).
- [4] P.J. Webster and K.R.A. Ziebeck. In: Alloys and Compounds of d-Elements with Main Group Elements. Part 2., Landolt-Börnstein, New Series, Group III, vol 19c, ed by H.R.J. Wijn, (Springer, Berlin 1988) pp 75–184.
- [5] K.R.A. Ziebeck and K.-U. Neumann. In: *Magnetic Properties of Metals*, Landolt-Börnstein, New Series, Group III, vol 32/c, ed by H.R.J. Wijn, (Springer, Berlin 2001) pp 64–414.
- [6] M. Gillessen, R. Dronskowski, J. Comput. Chem. 30 (2009) 1290.

- [7] M. Gillessen, R. Dronskowski, J. Comput. Chem. 31 (2010) 612.
- [8] J. Ma, V.I. Hegde, K. Munira, Y. Xie, S. Keshavarz, D.T. Mildebrath, C. Wolverton, A.W. Ghosh, W.H. Butler, Phys. Rev. B 95 (2017) 024411.
- [9] S.V. Faleev, Y. Ferrante, J. Jeong, M.G. Samant, B. Jones, S.S.P. Parkin Phys. Rev. B 95 (2017) 045140.
- [10] M.I. Katsnelson, V.Yu. Irkhin, L. Chioncel, A.I. Lichtenstein, R.A. de Groot, Rev. Mod. Phys. 80 (2008) 315.
- [11] I. Galanakis, P.H. Dederichs, N. Papanikolaou, Phys. Rev. B 66 (2002) 174429.
- [12] X.T. Wang, Z. Cheng, R. Guo, J. Wang, H. Rozale, L. Wang, Z. Yu, G. Liu, Mater. Chem. Phys. 193 (2017) 99; X.T. Wang, Y.T. Cui, X.F. Liu, G. D. Liu, J. Magn. Magn. Mater. 394 (2015) 50; X.T. Wang, X.F. Dai, L.Y. Wang, X.F. Liu, W.H. Wang, G.H. Wu, C.C. Tang, G.D. Liu, J. Magn. Magn. Mater. 378 (2015) 16.
- [13] "Heusler Alloys. Properties, Growth, Applications", C. Felser and A. Hirohata (Eds.), Springer Series in Materials Science Vol. 222, Springer International Publishing (2016).
- [14] J.S. Moodera, G.-X. Miao, T.S. Santos, Phys. Today 63 (2010) 46.
- [15] G.-X. Miao, M. Münzenberg, J.S. Moodera, Rep. Progr. Phys. 74 (2011) 036501.
- [16] P. LeClair, J.K. Ha, H.J.M. Swagten, J.T. Kohlhepp, C.H. van de Vin, W.J.M. de Jonge, Appl. Phys. Lett. 80 (2002) 625.
- [17] A.T. Filip, P. LeClair, C.J.P. Smits, J.T. Kohlhepp, H.J.M. Swagten, B. Koopmans, W.J.M. de Jonge, Appl. Phys. Lett. 81 (2002) 1815.
- [18] G.-X. Miao and J.S. Moodera, Phys. Rev. B 85 (2012)144424.
- [19] M. Müller, M. Luysberg, C.M. Schneider, Appl. Phys. Lett. 98 (2011) 142503.
- [20] Q.-F. Sun and X.C. Xie, Appl. Phys. Lett. 106 (2015) 182407.
- [21] P. Lukashev, P. Kharel, S. Gilbert, B. Staten, N. Hurley, R. Fuglsby, Y. Huh, S. Valloppilly, W. Zhang, K. Yang, R. Skomski, D.J. Sellmyer, Appl. Phys. Lett. 108 (2016) 141901.
- [22] S. Ouardi, G.H. Fecher, C. Felser, and J. Kübler, Phys. Rev. Lett. 110 (2013) 100401.
- [23] X.T. Wang, Z. Cheng, J. Wang, X.-L. Wang, G. Liu, J. Mater. Chem. C 4 (2016) 7176; X.T. Wang, Z.X. Cheng, J.L. Wang, H. Rozale, L.Y. Wang, Z.Y. Yu, J.T. Yang, G.D. Liu, J. Alloys Compd. 686 (2016) 549.

- [24] K. Özdoğan, E. Şaşıoğlu, I. Galanakis, J. Appl. Phys. 113 (2013) 193903.
- [25] V. Alijani, J. Winterlik, G.H. Fecher, S.S. Naghavi, C. Felser, Phys. Rev. B 83 (2011) 184428.
- [26] I. Galanakis, K. Özdoğan, E. Şaşıoğlu, Appl. Phys. Lett. 103 (2013) 142404.
- [27] I. Galanakis, K. Özdoğan, E. Şaşıoğlu, J. Phys.: Condens. Matter 26 (2014) 086003; ibid. 26 (2014) 379501(E).
- [28] K. Özdoğan, E. Şaşıoğlu, I. Galanakis, Comp. Mat. Sci. 110 (2015) 77.
- [29] I. Galanakis, K. Özdoğan, E. Şaşıoğlu, AIP Adv. 6 (2016) 055606.
- [30] A. Mauger and C. Godart, Phys. Rep. 141 (1986) 51.
- [31] J.S. Moodera, T.S. Santos, T. Nagahama, J. Phys.: Condens. Matter 19 (2007) 165202.
- [32] J.S. Moodera, X. Hao, G.A. Gibson, R. Meservey, Phys. Rev. Lett. 61 (1988) 637.
- [33] T. Nagahama, T.S. Santos, J.S. Moodera, Phys. Rev. Lett. 99 (2007) 016602.
- [34] G.M. Stephen, I. McDonald, B. Lejeune, L.H. Lewis, D. Heinman, Appl. Phys. Lett. 109 (2016) 242401.
- [35] X.L. Wang, Phys. Rev. Lett. 100 (2008) 156404.
- [36] X. Wang, G. Peleckis, C. Zhang, H. Kimura, S. Dou, Adv. Mat. 21 (2009) 2196.
- [37] D.H. Kim, J. Hwang, E. Lee, K.J. Lee, S.M. Choo, M.H. Jung, J. Baik, H.J. Shin, B. Kim, K. Kim, B.I. Min, J.-S. Kang, Appl. Phys. Lett. 104 (2014) 022411.
- [38] S.M. Choo, K.J. Lee, S.M. Park, J.B. Yoon, G.S. Park, C.-Y. You, and M. H. Jung, Appl. Phys. Lett. 106 (2015) 172404.
- [39] S. Skaftouros, K. Özdoğan, E. Şaşıoğlu, I. Galanakis, Phys. Rev. B 87 (2013) 024420.
- [40] G.D. Liu, X.F. Dai, H.Y. Liu, J.L. Chen, Y.X. Li, G. Xiao, G. H. Wu, Phys. Rev. B 77 (2008) 014424.
- [41] M. Meinert, J.-M. Schmalhorst, G. Reiss, J. Phys.: Condens. Matter 23 (2011) 116005.
- [42] M. Meinert, J. Schmalhorst, G. Reiss, J. Phys.: Condens. Matter 23(2011) 036001.

- [43] M.E. Jamer, B.A. Assaf, T. Devakul, D. Heiman, Appl. Phys. Lett. 103 (2013) 142403.
- [44] M.E. Jamer, B.A. Assaf, G.E. Sterbinsky, D.A. Arena, D. Heiman, J. Appl. Phys. 116 (2014) 213914.
- [45] G.Z. Xu, Y. Du, X.M. Zhang, H.G. Zhang, E.K. Liu, W.H. Wang, G.H. Wu, Appl. Phys. Lett. 104 (2014) 242408.
- [46] S. Skaftouros, K. Özdoğan, E. Şaşıoğlu, I. Galanakis, Appl. Phys. Lett. 102 (2013) 022402.
- [47] G.Z. Xu, E.K. Liu, Y. Du, G.J. Li, G.D. Liu, W.H. Wang, G.H. Wu, Europhys. Lett. 102 (2013) 17007.
- [48] G.Y. Gao, K.-L. Yao, Appl. Phys. Lett. 103 (2013) 232409.
- [49] H.Y. Jia, X.F. Dai, L.Y. Wang, R. Liu, X.T. Wang, P.P. Li, Y.T. Cui, G.D. Liu, AIP Adv. 4(2014) 047113.
- [50] L. Wollmann, S. Chadov, J. Kübler, C. Felser, Phys. Rev. B 90 (2014) 214420.
- [51] L. Bainsla, A.I. Mallick, M.M. Raja, A.K. Nigam, B.S.D.Ch.S. Varaprasad, Y.K. Takahashi, A. Alam, K.G. Suresh, K. Hono, Phys. Rev. B 91 (2015) 104408.
- [52] L. Bainsla, A.I. Mallick, M.M. Raja, A.A. Coelho, A.K. Nigam, D.D. Johnson, A. Alam, K.G. Suresh, Phys. Rev. B 92 (2015) 045201.
- [53] I. Galanakis, K. Özdoğan, E. Şaşıoğlu, S. Blügel, J. Appl. Phys. 115 (2014) 093908.
- [54] Y.J. Zhang, G.J. Li, E.K. Liu, J.L. Chen, W.H. Wang, G.H. Wu, J. Appl. Phys. 113 (2013) 123901.
- [55] J. Kudrnovský, V. Drchal, I. Turek, Phys. Rev. B 88 (2013) 014422.
- [56] A. Jakobsson, P. Mavropoulos, E. Şaşıoğlu, S. Blügel, M. Ležaić, B. Sanyal, I. Galanakis, Phys. Rev. B 91 (2015) 174439.
- [57] T.S. Santos, J.S. Moodera, K.V. Raman, E. Negusse, J. Holroyd, J. Dvorak, M. Liberati, Y.U. Idzerda, E. Arenholz, Phys. Rev. Lett. 101 (2008) 147201.
- [58] L. Hedin, Phys. Rev. 139 (1965) A796.
- [59] W. G. Aulbur, L. Jönsson, J.W. Wilkins, in Solid State Physics, Vol. 54, p. 1, edited by H. Ehrenreich and F. Spaepen (Academic, New York, 2000).

- [60] E. Şaşıoğlu, I. Galanakis, C. Friedrich, and S. Blügel, Phys. Rev. B 88 $(2013)\ 134402.$
- [61] C. Tsirogiannis and I. Galanakis, J. Magn. Magn. Mat. 393 (2015) 297
- [62] M. Meinert, C. Friedrich, G. Reiss, S. Blügel, Phys. Rev. B 86 (1012) 245115.
- [63] www.flapw.de
- [64] J.P. Perdew, K. Burke, M. Ernzerhof, Phys. Rev. Lett. 77 (1996) 3865.
- [65] C. Friedrich, S. Blügel, A. Schindlmayr, Phys. Rev. B 81 (2010) 125102.
- $[66]\,$ M. Tas, E. Şaşıoğlu, I. Galanakis, C. Friedrich, S. Blügel, Phys. Rev. B93~(2016)~195155.
- [67] M. Tas, E. Şaşıoğlu, C. Friedrich, S. Blügel, I. Galanakis, J. Appl. Phys. 121 (2017) 053903.
- [68] K. Koepernik and H. Eschrig, Phys. Rev. B 59 (1999) 1743.